

Effect of Crown Ether on Ion Currents through Synthetic Membranes Containing a Single Conically Shaped Nanopore

Elizabeth A. Heins, Lane A. Baker, Zuzanna S. Siwy, Miguel O. Mota, and Charles R. Martin*

Department of Chemistry and Center for Research at the Bio/Nano Interface, University of Florida, Gainesville, Florida 32611-7200

Received: May 5, 2005; In Final Form: August 5, 2005

Ion-current measurements were made on synthetic polymer membranes that contained a single conically shaped nanopore. This entailed placing an electrolyte solution on either side of the membrane, using an electrode placed in each solution to control the transmembrane potential, and measuring the resulting transmembrane ion current. The effect of the crown ether commonly called 18-crown-6 (18C6) on the measured ion current was investigated. Adding 18C6 to the electrolyte solution on one side of a conical nanopore membrane provides a way to rectify the ion current flowing through the nanopore. This chemical rectification is observed only when the cation of the electrolyte is complexed by 18C6 (e.g., K^+), and when the mouth diameter of the conical nanopore is of molecular dimensions, in this case ~ 1.5 nm. This chemical rectification can either augment or diminish the inherent electrostatic rectification observed with these small mouth-diameter nanopores. We have interpreted these results using a model based on the formation of a junction potential at the membrane–solution interface. This junction potential arises because the transference number for the K^+ –18C6 complex in bulk solution is larger than its transference number in the mouth of the conical nanopore.

Introduction

Living cells use protein nanopores and channels, embedded within the cell membrane, to communicate chemically and electrically with the extracellular environment.^{1,2} The protein channels open and close in response to stimuli such as a change in the transmembrane potential difference, the presence of a specific small-molecule ligand, or a mechanical stress on the cell.¹ There is currently tremendous research interest in developing abiotic nanopores that mimic these gating functions.^{3–6} The motivation for this research is that if such “smart” abiotic nanopores could be developed, they could lead to new approaches for biosensor design,^{7,8} and to new types of synthetic nanopore membranes for chemical and bioseparations.

We and others have been investigating synthetic polymer membranes that contain a single conically shaped nanopore and mimic the biological nanopores and channels.^{3–6,9} These conical nanopore membranes are prepared by the track-etch method,¹⁰ and the nanopores can have small-diameter openings (hereafter called the mouth of the nanopore) as small as 1–2 nm.^{3,11} We have shown that single conical nanopore membranes can mimic the ion-current rectification function of voltage-gated ion channels^{4–6} and the ligand-induced open/close function of ligand-gated ion channels.^{12,13}

Polymers such as poly(ethylene glycol)s and molecules such as crown ethers are often used to probe the transport properties of both the biological^{14–17} and abiotic⁵ nanopores. For example, the crown ether commonly called 18-crown-6 (18C6)¹⁸ (Figure 1a) has been used to study the transport properties of the α -hemolysin (α -HL) biological nanopore.¹⁵ These studies have suggested that because the diameter of the 18C6 molecule (1.15 nm)¹⁹ is comparable to the diameter of the lumen of this nanopore (1.4 nm),²⁰ 18C6 has a dramatic effect on the transport properties of the α -HL nanopore.¹⁵

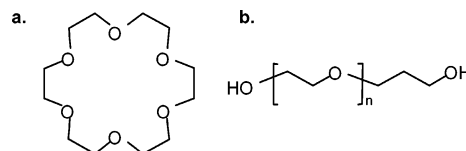


Figure 1. Structures of the molecules used to probe transport in the conical nanopores. (a) 1,4,7,10,13,16-Hexaoxacyclooctadecane (18C6). (b) Poly(ethylene glycol). For the $M_n \approx 200$ polymer used here (PEG200), n is ~ 4.2 .

We have been investigating the effect of 18C6 on the transport properties of conical nanopores with mouth diameters comparable to the lumen diameter of the α -HL nanopore. We have found that as with the biological nanopore, 18C6 dramatically changes the transport properties of such conically shaped abiotic nanopores. We demonstrate this by obtaining current–voltage curves associated with ion transport through the nanopore in the presence and absence of 18C6 in one of the electrolyte solutions contacting the nanopore membrane. The key result is that as with the biological nanopore,¹⁵ 18C6 can dramatically lower the ion current flowing through the nanopore. It is tempting to interpret this result in terms of occlusion of the nanopore by the 18C6.¹⁵ However, we believe that the mechanism is instead electrostatic in origin, and entails the formation of a junction potential²¹ at the membrane–solution interface. We report the results of these experiments, and the junction-potential based model used to interpret these results, here.

Experimental Section

Materials. Polyimide films (Kapton-50HN, Du Pont, 3 cm diameter, 12 μ m thick) that had been irradiated with a single swift, heavy ion of 2.2 GeV of kinetic energy to create a single damage track through the film were obtained from GSI, Darmstadt, Germany. KCl and KI (certified ACS, Fisher Scientific), 1,4,7,10,13,16-hexaoxacyclooctadecane or 18-crown-6 (18C6, 99%, Sigma), poly(ethylene glycol) (PEG200,

* To whom correspondence should be addressed. E-mail: crmartin@chem.ufl.edu. Fax: 352-392-8206. Voice: 352-392-8205.

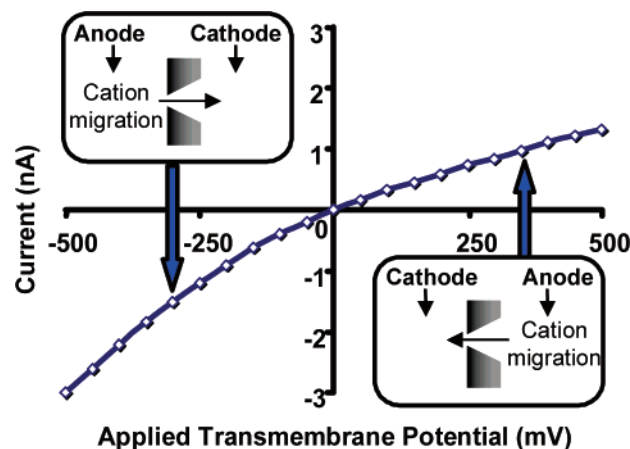


Figure 2. Current–voltage curve for a conical nanopore with mouth diameter ~ 1.5 nm in 1 M KCl, pH = 8.

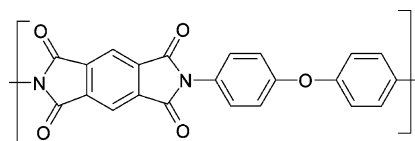
$M_n = 200$ Da), sodium hypochlorite (13% active chloride ion, Sigma), and lithium chloride (99%, Acros) were used as received. All solutions were prepared in 18 M Ω water (Barnstead, E-pure).

Preparation of the Conical Nanopores. Membrane samples that contained a single conically shaped nanopore were prepared by anisotropic chemical etching of the heavy-ion irradiated Kapton films. As per the procedure developed by Apel et al., the irradiated film was placed between the two halves of a conductivity cell, and an etch solution (sodium hypochlorite) was added to one half-cell and a stop solution (1 M KI) to the other half-cell.^{11,22} Each half-cell contained a Pt wire, and a transmembrane potential difference of 1 V was applied during etching using a Keithley 6487 picoammeter/voltage source (Keithley Instruments, Cleveland, OH).

The progress of the etching process can be monitored by measuring the transmembrane current during etching.²² Etching was halted when a transmembrane current of 50 pA was measured. The membrane was then removed from the conductivity cell and placed in water overnight. We will refer here to the large-diameter opening of the conical nanopore as the “base” of the nanopore and the small opening as the “mouth” of the nanopore. All of the nanopores studied here had a base diameter, d_{base} , of 2 μm , as measured using scanning electron microscopy. The mouth diameter, d_{mouth} , was determined electrochemically (vide infra). The etch process also thinned the membrane from 12 to 10 μm .

Electrochemical Measurements. The single conical nanopore membrane was mounted in a conductivity cell, and both half-cells were filled with electrolyte solution. For most of our studies, the electrolyte added to both half-cells was 1 M KCl, brought to pH 8 with phosphate buffer, but some experiments were done with 1 M LiCl. A Ag/AgCl electrode was inserted into each half-cell solution, and the Keithley picoammeter/voltage source was used to obtain current–voltage curves associated with ionic migration through the nanopore. The working Ag/AgCl electrode was in the half-cell solution facing the base of the nanopore, and the reference Ag/AgCl electrode was in the half-cell solution facing the nanopore mouth. Current–voltage curves were obtained by stepping the voltage in 50 mV increments from -500 to $+500$ mV at a rate of 5 s per step. The sign convention is as follows: A positive transmembrane potential means that the working electrode is the anode, and a negative transmembrane potential means that the working electrode is the cathode (insets, Figure 2). The

SCHEME 1



current–voltage curves reported here are averages of three sequential measurements made on the same nanopore.

Current–time recordings were performed with a single conical nanopore membrane mounted in a conductivity cell as described above. Recordings were obtained using an Axopatch 200B current amplifier (Molecular Devices Corporation, Union City, CA) in the voltage-clamp mode with a low-pass Bessel filter at 2 kHz bandwidth. The signal was further digitized using a Digidata 1233A analog-to-digital converter (Molecular Devices Corporation). Data were recorded and analyzed using pClamp 9.0 software (Molecular Devices Corporation).

Estimation of the Mouth Diameter, d_{mouth} . The ionic resistance of an electrolyte-filled conically shaped pore is given by²²

$$R = \frac{4\rho l}{\pi d_{\text{base}} d_{\text{mouth}}} \quad (1)$$

where ρ is the specific resistance of the electrolyte and l is the length of the pore, in this case the membrane thickness, 10 μm . R was determined from the experimental current–voltage curves, and was used to calculate d_{mouth} . However, as will be discussed below, the current–voltage curves for these conical nanopores are nonlinear (e.g., Figure 2). For the reasons discussed by Apel et al. we use the currents obtained between -200 and $+200$ mV to obtain R .²² The specific resistance values for the electrolytes were measured using a YSI conductivity meter (Yellow Springs, OH). Values of 10 and 15 $\Omega \text{ cm}$ were obtained for 1 M KCl and 1 M LiCl, respectively. Most of our studies were done with nanopores having $d_{\text{mouth}} \approx 1.5$ nm.

Results and Discussion

Chemistry and Charge of the Polyimide Nanopore. The chemical structure of the polyimide used here is shown in Scheme 1. When etched with sodium hypochlorite and then exposed to solutions with pH = 8, as used here, the surface of this initially electrically neutral polymer becomes negatively charged.²³ This negative surface charge can be removed by exposure to solutions with pH ≤ 3 , suggesting, in accord with the chemical structure, that the negative surface charge is due to deprotonated carboxylate groups.^{3,23} The maximum surface charge, obtained at pH ≥ 9 , has been determined to be approximately 1.5 negative charges per nm².²⁴

As a result of this surface charge, the nanopores are cation-permselective, provided the mouth diameter is small relative to the Debye screening length for the electrolyte solution employed.²⁵ This means that current is carried through the nanopore predominately by cations, which as we will see, simplifies the interpretation of the current–voltage curves for these nanopores. Furthermore, such cation-permselective conical nanopores show nonlinear (rectifying) current–voltage curves; i.e., for any absolute value of applied transmembrane potential, the current is higher at negative potentials than at the equivalent positive potentials (Figure 2). As discussed in detail previously,^{4,26} this is because cations migrating from base to mouth experience an electrostatic trap not observed when cations are migrating from mouth to base.

Soluble Polyethers as Probes of Nanopores. Soluble polymers, such as poly(ethylene glycol)s (PEGs, Figure 1b), are often used to characterize biological nanopores. For example, current-noise analyses were used to study the interactions between PEGs and the α -hemolysin (α -HL) nanopore.^{14,16} PEG molecules of size comparable to the diameter of the lumen of α -HL produced increased noise due to chemical interaction between the PEG and the nanopore walls.

The cyclic polyether 18C6¹⁸ (Figure 1a) has also been used to study α -HL.¹⁵ 18C6 is an uncharged molecule with an outer diameter of approximately 1.15 nm.¹⁹ Because of the available lone pairs on the ether oxygens, crown ethers complex cations, and the complex retains the positive charge of the complexed cation. The potassium cation is complexed by 18C6 with a formation constant of approximately 100 M^{-1} in aqueous solution.²⁷ In contrast, the formation constant between Li^+ and 18C6 in aqueous solution is effectively zero.²⁸ We have used 18C6 in the presence of both KCl and LiCl electrolyte solutions to investigate our polyimide conical nanopores.

Effect of 18C6 on Current–Voltage Curves with KCl as the Electrolyte. 18C6 was added to one of the half-cell solutions, and current–voltage curves were obtained as a function of concentration of the added 18C6. Fresh electrolyte was then added to that half-cell, and the experiments were repeated with 18C6 added to the other half-cell. The concentration range of 18C6 used was 5 to 50 mM. Because of the large formation constant between K^+ and 18C6, and because of the large excess of free K^+ , essentially all of the added 18C6 is present in the solution as the positively charged $\text{K}^+-18\text{C6}$ complex.

Figure 3a shows current–voltage curves with the 18C6 added to the solution facing the mouth ($d_{\text{mouth}} \approx 1.5\text{ nm}$) of the conical nanopore. At positive applied transmembrane potentials, the positively charged $\text{K}^+-18\text{C6}$ complex is driven electrophoretically away from the membrane surface, and the 18C6 has no effect on the current–voltage curve. Charge is carried through the nanopore by free K^+ ions migrating from base to mouth (upper inset, Figure 3a). At negative applied transmembrane potentials, both the excess uncomplexed K^+ and the positively charged $\text{K}^+-18\text{C6}$ complex are driven electrophoretically into the mouth of the nanopore (lower inset, Figure 3a). In this case, the measured current at any applied potential decreases with an increasing concentration of 18C6.

Figure 3b shows analogous current–voltage curves for 18C6 added to the solution facing the base of the conical nanopore. At negative applied transmembrane potentials, the positively charged $\text{K}^+-18\text{C6}$ complex is driven electrophoretically away from the membrane surface, and the 18C6 has no effect on the current–voltage curve. Charge is carried through the nanopore by free K^+ ions migrating from mouth to base (upper inset, Figure 3b). At positive applied transmembrane potentials, both the excess uncomplexed K^+ and the positively charged $\text{K}^+-18\text{C6}$ complex are driven electrophoretically into the mouth of the nanopore (lower inset, Figure 3b). Again, we find that when the complex is driven into the nanopore, the measured current at any applied potential decreases with an increasing concentration of 18C6.

In summary, Figure 3 shows that when the $\text{K}^+-18\text{C6}$ complex is driven electrophoretically into the nanopore, the current decreases with an increasing 18C6 concentration, and this is true whether the complex is driven into the nanopore from mouth to base (Figure 3a) or from base to mouth (Figure 3b). For these experiments, d_{mouth} (1.5 nm) is comparable to the diameter of the 18C6 complex (1.15 nm). Figure 4 shows

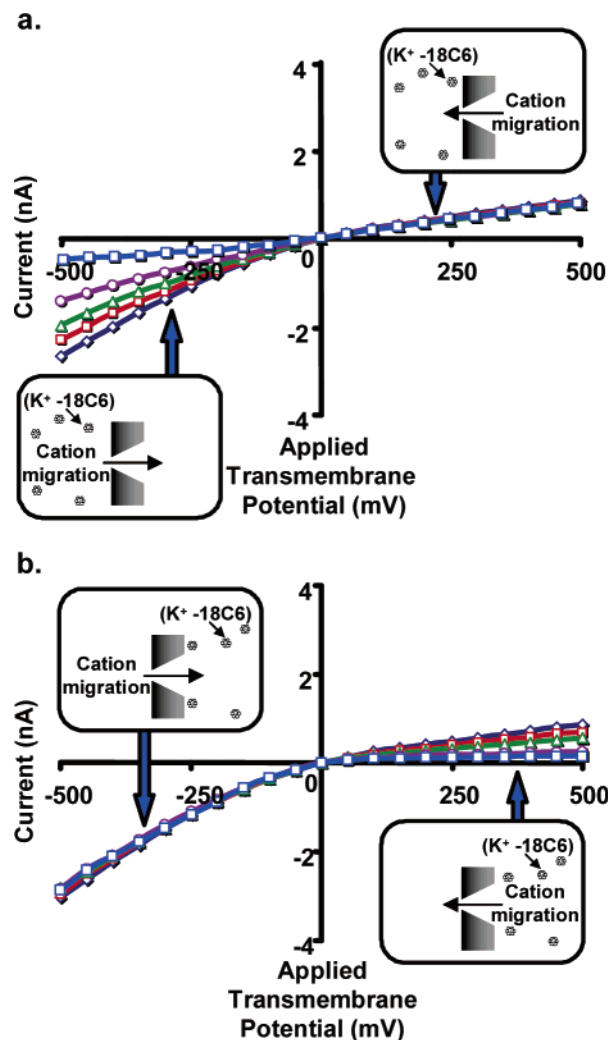


Figure 3. Current–voltage curves for a conical nanopore with mouth diameter $\sim 1.5\text{ nm}$, and with 18C6 added to the 1 M KCl solution facing the mouth (a) or base (b) of the conical nanopore. The concentration of 18C6 was 0 mM (\diamond), 5 mM (\square), 10 mM (\triangle), 25 mM (\circ), or 50 mM (\square). Each data point is the average of three replicate measurements on the same membrane. The standard deviation is $\sim 2\%$ of the measured average current. Error bars are not shown because they are approximately equivalent to the width of the lines in the plot.

analogous current–voltage curves for a nanopore with $d_{\text{mouth}} \approx 3\text{ nm}$. 18C6 has essentially no effect on the current–voltage curve for this larger mouth-diameter nanotube regardless of the polarity of the applied potential, the electrolyte solution to which the 18C6 is added, and the 18C6 concentration. Similar results were obtained for nanopores with $d_{\text{mouth}} \approx 9$ and 15 nm .

These studies show that for 18C6 to have an effect on the current–voltage curve, the nanopore must have a mouth diameter comparable to that of the 18C6 molecule. These studies also discount an alternative possibility, that the small amount of complexed K^+ produces a large decrease in the conductivity of the 1 M KCl solution. If this were the case, 18C6 would decrease the observed current regardless of the mouth diameter of the nanopore, and this is not what is observed experimentally. Furthermore, independent measurements of the conductivities of the various solutions used here confirm that this is not the case.

Effect of 18C6 on Current–Voltage Curves with LiCl as the Electrolyte. We have suggested that electrophoretic transport of the large $\text{K}^+-18\text{C6}$ complex into the nanopore is responsible for the observed effects of added 18C6 on the

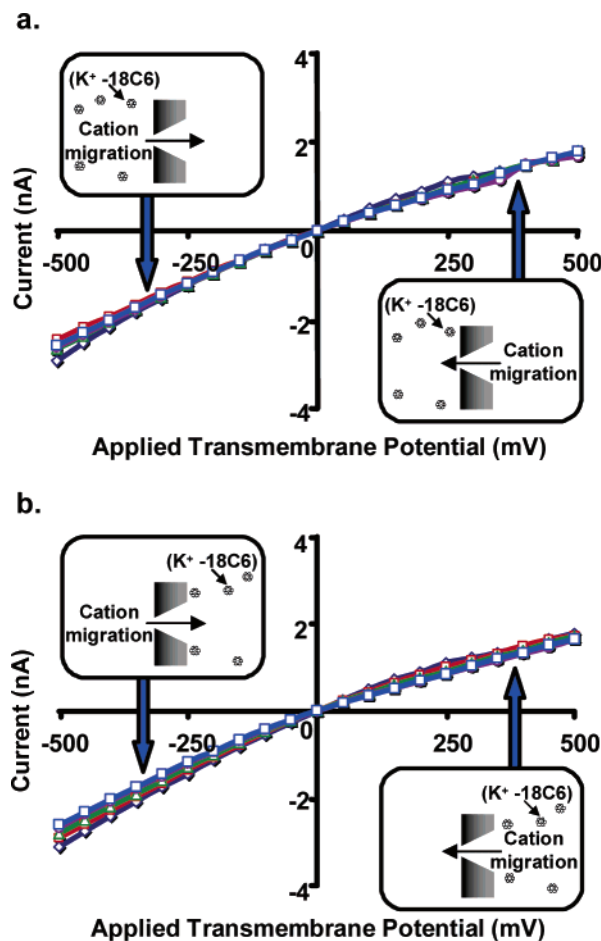


Figure 4. Current–voltage curves for a conical nanopore with mouth diameter ~ 3.0 nm, and with 18C6 added to the 1 M KCl solution facing the mouth (a) or base (b) of the conical nanopore. The concentration of 18C6 was 0 mM (\diamond), 5 mM (\square), 10 mM (\triangle), 25 mM (\circ), or 50 mM (\square). Each data point is the average of three replicate measurements on the same membrane.

current–voltage curves (Figure 3). It seemed possible, however, that simple diffusion-based transport of the 18C6 into the nanopore might be sufficient to produce the effects observed here. To discount this possibility, we have performed analogous experiments using LiCl as the electrolyte. Because Li^+ is not complexed by 18C6,²⁸ the crown is not electrophoretically driven into the nanopore. The crown is, however, free to diffuse into the nanopore. The results of these experiments using a nanopore with $d_{\text{mouth}} \approx 1.5$ nm and the highest 18C6 concentration (50 mM) are shown in Figure 5. Addition of 18C6 has no effect on the current–voltage curves regardless of the side of the membrane to which it is added or the polarity of the applied potential.

This experiment also eliminates the possibility that 18C6 has some special chemical affinity with the nanopore, and that it is this chemical effect that is responsible for the results in Figure 3. Finally, it is also possible that the effects in Figure 3 are due to transport of the $\text{K}^+ - 18\text{C6}$ complex into the nanopore via electro-osmotic flow (EOF²⁹) as opposed to the electrophoretic mechanism³⁰ proposed here. Since the nanopore has negative surface charge, EOF-based transport is in the same direction as electrophoretic transport. However, EOF does not require that the species being transported be charged.²⁹ Hence, if the dominant transport mechanism driving the 18C6 into the nanopore was EOF, the results in KCl and LiCl would be the same, and this is not what is observed experimentally.

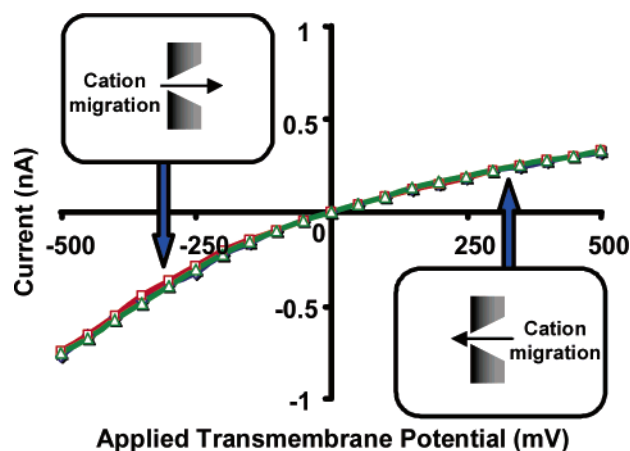


Figure 5. Current–voltage curves for a conical nanopore with mouth diameter ~ 1.5 nm, and with 1 M LiCl as the electrolyte. (\diamond) 1 M LiCl, no added 18C6. (\square) 1 M LiCl and 50 mM 18C6 added to the solution facing the mouth of the nanopore. (\triangle) 1 M LiCl and 50 mM 18C6 added to the solution facing the base of the nanopore.

Effect of PEG200 on the Current–Voltage Curve with KCl as the Electrolyte. To further confirm that electrophoretic transport of the $\text{K}^+ - 18\text{C6}$ complex into the nanopore is responsible for the changes in the current–voltage curves observed in Figure 3, we conducted analogous experiments with a linear poly(ethylene glycol), PEG200 (Figure 1b, $n \approx 4.2$). The molecular mass of PEG200 (~ 200 Da) is similar to that of 18C6 (264 Da). PEG200 is also similar to 18C6 in that both contain ether functionalities. There are approximately 4 ether functionalities per PEG200 molecule. However, PEG200 and 18C6 are different in that PEG200 is a linear molecule and 18C6 is cyclic. Since PEG200 is linear, it does not form stable complexes with metal ions, and remains uncharged in a solution of KCl.³¹ Therefore, PEG200 is not electrophoretically driven into the nanopore, and in analogy to the LiCl experiments, PEG200 has essentially no effect on the current–voltage curve, regardless of concentration, face of the membrane to which it is added, or polarity of the transmembrane potential (Figure 6a and 6b).

Effect of 18C6 on the Extent of Rectification. As noted earlier, conical nanopores that have excess surface charge and a small mouth diameter relative to the Debye screening length act as ion-current rectifiers.^{4,26} This is because cations migrating from base to mouth experience an electrostatic trap not observed when cations are migrating from mouth to base.⁴ As a result, in the absence of 18C6, higher currents are observed at any given negative transmembrane potential relative to the current observed at the same positive transmembrane potential (Figure 2). The extent of rectification can be quantified via the ratio r

$$r = \left| \frac{i_{-500}}{i_{+500}} \right| \quad (2)$$

where i_{-500} is the current at an applied transmembrane potential of -500 mV and i_{+500} is the current at $+500$ mV. In the absence of 18C6, this intrinsic electrostatic rectification yields an r value of 3.1.

The addition of 18C6 provides a means to tune the rectifying properties of the nanopore. This is because when added to only one side of the membrane, as described here, 18C6 affects only one branch (positive currents or negative currents) of the current–voltage curve. Hence 18C6 also rectifies the ion current, and this transport-induced rectification can either add to (Figure 3b) or subtract from (Figure 3a) the intrinsic electrostatic

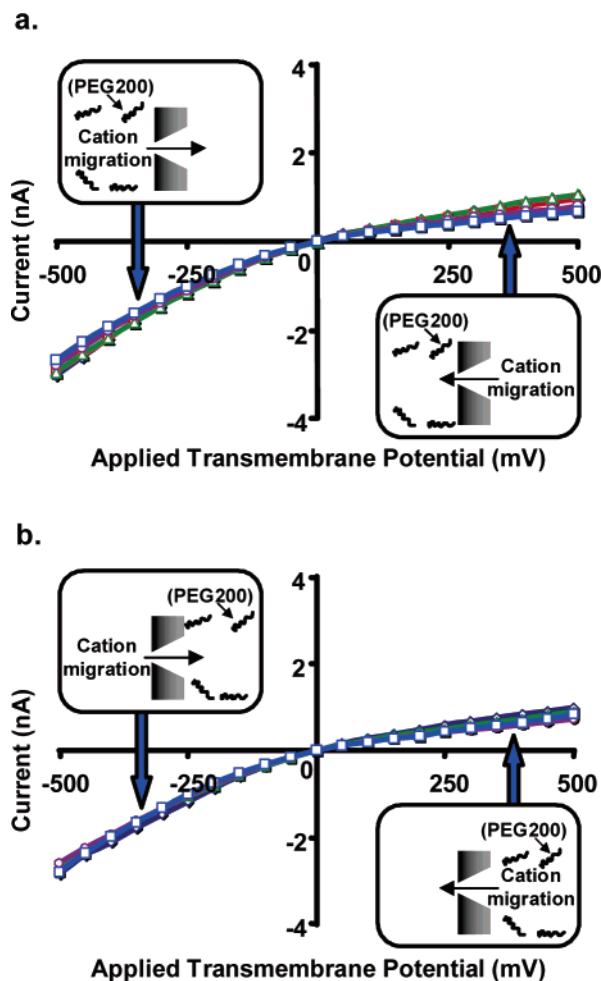


Figure 6. Current–voltage curves for a conical nanopore with mouth diameter ~ 1.5 nm, and with PEG200 added to the 1 M KCl solution facing the mouth (a) or base (b) of the conical nanopore. The concentration of PEG200 was 0 mM (\diamond), 5 mM (\square), 10 mM (\triangle), 25 mM (\circ), or 50 mM (\square).

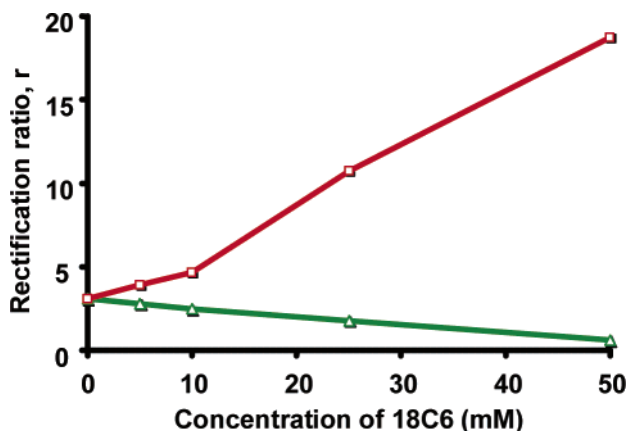


Figure 7. Rectification ratio, r (eq 2), vs concentration of added 18C6 for a conical nanopore with mouth diameter ~ 1.5 nm. 18C6 was added to the 1 M KCl solution facing the mouth (\square) or base (\triangle) of the nanopore.

rectification of the nanopore, depending on the side of the nanopore to which the 18C6 is added. This is shown in Figure 7 as plots of r (eq 2) vs concentration of crown added to the solution facing either the base or the mouth of the conical nanopore.

When 18C6 is added to the side of the membrane facing the base of the nanopore, the transport-induced rectification adds

to the intrinsic electrostatic rectification (upper curve in Figure 7). At the maximum concentration of 18C6 (50 mM), an r value of 18.8 is obtained, 6 times larger than the value produced by the intrinsic electrostatic rectification. When 18C6 is added to the side of the membrane facing the mouth of the nanopore, the transport-induced rectification subtracts from the intrinsic electrostatic rectification (lower curve in Figure 7). At the maximum concentration of 18C6, an r value of 0.6 is obtained, 5 times smaller than the value produced by the intrinsic electrostatic rectification. Furthermore, the fact that r is less than unity indicates that the transport-induced rectification supplants the intrinsic electrostatic rectification.

Model. 18C6 has been used as a probe to study ion transport in the α -HL biological nanopore,¹⁵ and results similar to those reported here were obtained. Most importantly, in agreement with our results, the ion current carried through the α -HL nanopore was observed to decrease when 18C6 was added to the contacting KCl electrolyte solution.¹⁵ One way to interpret these results is to assume that the bulky K^+ –18C6 complex trapped in the narrowest part of the nanopore partially occludes the pathways used by the more mobile free K^+ ions to transport charge through the nanopore.

We initially considered this “occlusion-based” model, which can be explained most easily by considering the case in which the K^+ –18C6 complex is being driven electrophoretically from the base into the mouth of the nanopore, as illustrated in the lower inset of Figure 3b. Because the nanopore mouth and the K^+ –18C6 complex have comparable diameters, the diffusion coefficient associated with transport of the complex through the mouth of the nanopore will be strongly hindered.³² Indeed the theory of hindered diffusion indicates that the diffusion coefficient for the K^+ –18C6 complex in the mouth of a nanopore with $d_{\text{mouth}} \approx 1.5$ nm will be approximately 2 orders of magnitude smaller than the diffusion coefficient for the complex in bulk solution.³² As a result, when the K^+ –18C6 complex is driven electrophoretically in at the base, it gets caught in the mouth, producing a locally higher concentration of the complex just inside the mouth of the nanopore.

The occlusion-based model would then suggest that in analogy to the Coulter counter,³³ the K^+ –18C6 complex caught in the mouth of the nanopore partially occludes the pathways which the smaller and more mobile free K^+ ions use to carry charge through the nanopore. As a result, in agreement with the experimental data (Figure 3), the ionic resistance of the nanopore would go up, and the transmembrane current would go down. Furthermore, it seems reasonable to suggest that the higher the concentration of the K^+ –18C6 complex in the bulk solution, the higher the local concentration of complex trapped in the nanopore mouth. As a result, the transmembrane current would decrease with an increasing concentration of the K^+ –18C6 complex, again in agreement with the experimental data.

The main problem with this model is that the K^+ –18C6 complex is positively charged, and building up a high local concentration of charge in any region of solution is a violation of electroneutrality. To appreciate the consequences of this violation, it is instructive to consider a simple analogue, the interface between two solutions that have the same dissolved electrolyte (e.g., HCl) but at two different concentrations.²¹ In this situation, both H^+ and Cl^- move from the high-concentration solution, across the interface, and into the low-concentration solution. However, because H^+ is more mobile, the region adjacent to the interface in the low-concentration solution has $[\text{H}^+] > [\text{Cl}^-]$, and the region adjacent to the interface in the high-concentration solution has $[\text{H}^+] < [\text{Cl}^-]$. That is, electro-

neutrality is violated on a very localized scale on both sides of the interface. The consequence of this violation is that a junction potential develops at the interface.²¹ This junction potential impedes H^+ transport and accelerates Cl^- transport across the interface. Hence the junction potential allows mixing to occur without the electroneutrality violation propagating into the bulk solutions.

In analogy to this example, we propose that electrophoretic transport of the positively charged K^+-18C6 complex into the nanopore results in a local violation of electroneutrality at the nanopore mouth. This causes a junction potential to develop, and the sign of this junction potential is such that it opposes the applied transmembrane potential. As a result, the junction potential decreases the driving force for electrophoretic transport of cations through the nanopore, and this prevents the electroneutrality violation from propagating. Furthermore, because the junction potential opposes the applied transmembrane potential, the ion current carried by the nanopore decreases in the presence of 18C6, in agreement with the experimental data.

To develop this model we assume (as per our experiment) the following: (1) KCl solution (1 M) is in contact with both faces of a single conical nanopore membrane with mouth diameter = 1.5 nm. (2) 18C6 (50 mM) is added to the solution facing the nanopore mouth, as per the lower inset in Figure 3a. (3) In this solution, the concentration of the K^+-18C6 complex (C_{comp}) is essentially 50 mM, and the concentration of free K^+ ion (C_{free}) is 0.95 M. (4) A transmembrane potential difference is applied such that cations (both free K^+ and the K^+-18C6 complex) are driven electrophoretically from the bulk solution into the nanopore mouth, again as per the lower inset in Figure 3a. (5) The ion current in bulk solution is carried by both anions and cations. (6) The conical nanopore is ideally cation permselective with a cation transference, t^+ , of 1.

In bulk solution, the following equations hold true

$$t_{free} + t_{comp} + t_{Cl} = 1 \quad (3)$$

$$i_{free} = t_{free} i_{tot} \quad (4)$$

$$i_{comp} = t_{comp} i_{tot} \quad (5)$$

where t_{free} , t_{Cl} , and t_{comp} are the transference numbers for the free K^+ ion, the Cl^- ion, and the K^+-18C6 complex, respectively; i_{tot} is the measured total current; and i_{free} and i_{comp} are the currents carried by the free K^+ ion and the K^+-18C6 complex, respectively.

Our objective is to calculate i_{free} and i_{comp} in the bulk electrolyte solution, and in the solution just inside the mouth of the conical nanopore. To do this we must assume a value for i_{tot} ; in accord with the experimental data (see, e.g., Figure 3a), we assume $i_{tot} = 1$ nA. We begin by calculating the transference numbers, but as we will see, the transference numbers in bulk solution and in the solution just inside the mouth of the nanopore are different. Considering the bulk-solution case first, and noting that all ions involved are monovalent, we calculate the transference number for the complex via

$$t_{comp} = \frac{\mu_{comp} C_{comp}}{\mu_{free} C_{free} + \mu_{comp} C_{comp} + \mu_{Cl} C_{Cl}} \quad (6)$$

where μ is the electrophoretic mobility for the indicated ion and C is the concentration.³⁴ The mobility for any monovalent ion, i , is given by³⁴

$$\mu_i = \frac{e}{6\pi\eta r} \quad (7)$$

where e is the electronic charge, η is the solution viscosity, and r is the radius of the ion. The radius of the hydrated free K^+ ion is $r_{free} \approx 0.15$ nm;³⁵ the radius of the hydrated free Cl^- is $r_{Cl} \approx 0.15$ nm;³⁵ and the radius of the K^+-18C6 complex is $r_{comp} = 0.575$ nm.¹⁹ Combining eqs 6 and 7 with these numbers yields $t_{comp,BK} = 0.007$, $t_{free,BK} = 0.509$, and $t_{Cl, BK} = 0.484$. We have added the subscript BK to denote that these are the transference numbers for these ions in the bulk solution. Using these numbers in eqs 4 and 5 with $i_{tot} = 1$ nA gives $i_{comp,BK} = 0.007$ nA, $i_{free,BK} = 0.509$ nA, and $i_{Cl, BK} = 0.484$ nA.

As discussed above, the theory of hindered diffusion indicates that the diffusion coefficient for the complex in the mouth of the nanopore will be at least 2 orders of magnitude smaller than the diffusion coefficient for the complex in bulk solution.³² This difference in diffusion coefficient for the complex between the bulk solution and the mouth of the nanopore makes the bulk-solution vs nanopore transference numbers different, and it is this difference in transference numbers that leads to the junction potential.

To calculate the transference numbers in the mouth of the nanopore, we note that for any monovalent ion, i , the Stokes–Einstein equation provides the following relationship between μ_i and the diffusion coefficient, D_i

$$\mu_i = \frac{eD_i}{kT} \quad (8)$$

We also assume that because the pore is selective for cations, the transference number for Cl^- in the pore is zero. Substituting eq 8 into eq 6 yields

$$t_{comp,NP} = \frac{\left(\frac{C_{comp}eD_{comp,NP}}{kT}\right)}{\left(\frac{C_{free}eD_{free,NP}}{kT}\right) + \left(\frac{C_{comp}eD_{comp,NP}}{kT}\right)} \quad (9)$$

The subscript NP denotes that these are the diffusion coefficients and transference number in the solution just inside the mouth of the nanopore. We assume that because of its small size, the diffusion coefficient for the free K^+ ion is not hindered in the nanopore mouth and that because of its larger size, the diffusion coefficient for the K^+-18C6 complex is 2 orders of magnitude smaller than this value.³² Furthermore, we assume that the concentration of the K^+-18C6 complex is uniform everywhere in the electrolyte solution ($C_{comp} = 50$ mM), which, as we will discuss further below, will only be rigorously true at the start of an ion-current measurement.

Plugging these various values into eq 9 yields $t_{comp,NP} = 1.37 \times 10^{-4}$. The transference number for free K^+ in the nanopore is the difference $(1 - t_{comp,NP})$, meaning $t_{free,NP}$ is effectively unity. Using these numbers in eqs 3 and 4 with $i_{tot} = 1$ nA gives $i_{comp,NP} = 1.37 \times 10^{-4}$ nA and $i_{free,NP} \approx 1.0$ nA. We find that in the bulk solution, the K^+-18C6 complex carries 0.007 nA of the total 1 nA ion current, but because the diffusion coefficient plummets in the mouth of the nanopore, the complex can carry only 1.37×10^{-4} nA of the current within the nanopore. This means that the K^+-18C6 complex is *initially* being transported to the mouth of the nanopore at a higher rate than it can be cleared through the nanopore, and as a result, the local concentration of the K^+-18C6 complex in the solution adjacent to the nanopore mouth increases above the bulk value.

As noted above, this constitutes a violation of electroneutrality, and a junction potential develops. Because this junction potential is caused by accumulated cations (the K^+ –18C6 complex), it repels cations from the face of the membrane. Since the applied transmembrane potential pushes cations toward the face of the membrane (lower inset in Figure 3a), the junction potential opposes the applied transmembrane potential. As a result, when 18C6 is added to the solution facing the mouth of the nanopore, the net field strength available to drive cations across the membrane goes down, and the measured current decreases.

This prediction of the model—that the measured current decreases when 18C6 is added—is one of our key experimental results (e.g., Figure 3). Furthermore, as the concentration of the K^+ –18C6 complex increases, its transference number in solution increases, which means that a larger quantity of the complex will accumulate at the nanopore mouth. As a result, the junction potential opposing cation transport will increase with an increasing concentration of the K^+ –18C6 complex, and so the measured current decreases with an increasing concentration of the complex. Again, this prediction of the model is one of our key experimental results.

Although there is no doubt that this situation leads to a junction potential that opposes cation transport across the membrane, the key question is whether this junction potential will be large relative to the applied transmembrane potential difference. To answer this question, we assume that the applied transmembrane potential difference is 0.5 V, the largest value used in our experimental work; i.e., this is the worst case scenario in terms of the junction potential opposing the applied transmembrane potential. Next we need a measure of the rate at which the K^+ –18C6 complex accumulates in the electrolyte solution adjacent to the nanopore mouth. In the short time limit (*vide infra*), the rate at which complex approaches the nanopore mouth is given by $i_{\text{comp,BK}} = 0.007$ nA, and the rate at which the complex is cleared by the nanopore is given by $i_{\text{comp,NP}} = 1.37 \times 10^{-4}$ nA. Hence the rate at which the complex accumulates is simply the difference between these two currents, $\Delta i = 6.86 \times 10^{-3}$ nA.

We then ask the following question: At this $\Delta i = 6.86 \times 10^{-3}$ nA rate, how long would it take for the excess charge accumulating at the mouth of the nanopore (due to the K^+ –18C6 complex) to develop a junction potential equivalent to the applied transmembrane potential difference of 0.5 V? This time, t , can be obtained by drawing an analogy to the charging of the electrical double layer at an electrode–solution interface.³⁶ If the electrode potential is initially the potential of zero charge (no excess charge on the electrode surface), the transient part of the double-layer charging process is given by eq 10³⁶

$$E = \frac{\Delta i t}{C_{\text{dl}} A} \quad (10)$$

where E is the potential, Δi is the current, C_{dl} (Farads cm^{-2}) is the double layer capacitance, and A is the electrode area.

In the electrochemical experiment, excess charge is accumulating at the electrode–solution interface because of the applied current, i . In our experiment, excess charge is accumulating at the membrane/solution interface because of the difference current $\Delta i = 6.86 \times 10^{-3}$ nA. Hence eq 10 is directly applicable to our experiment provided we have a value for the capacitance of the membrane–solution interface and a value for the area of the membrane surface where the excess charge is accumulating. We began our calculations using a capacitance of $1 \mu\text{F cm}^{-2}$,^{37,38} but as we will see, this value can be changed

by many orders of magnitude without changing the primary conclusion, that a junction potential of 0.5 V (eq 10) very rapidly develops in our experiment.

To obtain a value for the area of the membrane surface where the excess charge is accumulating, A_{eff} , we draw an analogy between the K^+ –18C6 complex that accumulates in the solution adjacent to the mouth of the nanopore and the concentration gradient that develops at a disk-shaped ultramicroelectrode³⁹ with a radius, r_{elect} , equivalent to $r_{\text{mouth}} = 0.75$ nm. If the reduction $\text{Ox} + e^- \rightarrow \text{Red}$ is occurring at the ultramicroelectrode, then Red accumulates in the solution adjacent to the electrode surface just as the K^+ –18C6 complex accumulates in the solution adjacent to the disk-shaped mouth of our nanopore. A hemispherical diffusion layer develops at the electrode surface, and the radius of this diffusion layer is $\sim 10r_{\text{elect}}$.⁴⁰ We assume that same relationship holds for the diffusion layer of the K^+ –18C6 complex created at the mouth of our nanopore. Hence the effective radius of the diffusion layer for the K^+ –18C6 complex at the nanopore surface is ~ 7.5 nm, making $A_{\text{eff}} \approx 1.8 \times 10^{-12}$ cm^2 .

Plugging these values for C_{dl} and A_{eff} into eq 10 shows that a junction potential of 0.5 V develops in $\sim 1 \mu\text{s}$. The relevant time scale for our experiment is the 5 s time interval we wait at each applied transmembrane potential before taking a measurement of the transmembrane ion current (see Experimental Section). Hence, as noted above, even if the approximations we use for C_{dl} and A_{eff} are off by 6 orders of magnitude, we reach the same conclusion—a substantial junction potential develops at the membrane–solution interface for the 18C6 concentrations and time scales used in our experiments.

We can now refine the model. Clearly, accumulation of the K^+ –18C6 complex does not proceed unabated for the entire 5 s that we apply any given transmembrane potential difference. If this happened, the junction potential would be 25 mV (eq 10). What does happen? The answer is 3-fold. First, as is shown by our experimental data, the junction potential causes the current to decrease, and as a result, $i_{\text{comp,BK}}$ (the rate at which the K^+ –18C6 complex is supplied to the nanopore) decreases. Second, the accumulation of the K^+ –18C6 complex in the solution adjacent to the nanopore mouth raises the local concentration, and this increases the transference number for the complex at the nanopore mouth. As a result, $i_{\text{comp,NP}}$ (the rate at which the complex is cleared by the nanopore) increases. Finally, we must also consider back diffusion of the accumulated K^+ –18C6 complex away from the nanopore mouth. As the concentration of the complex in the solution adjacent to the nanopore mouth increases, the rate of back diffusion of complex into the bulk solution increases. For all three of these reasons, $i_{\text{comp,BK}}$ ultimately becomes equal to $i_{\text{comp,NP}}$, and an enhanced steady-state (relative to bulk) local concentration of the K^+ –18C6 complex is achieved. This enhanced steady-state concentration of the K^+ –18C6 complex yields a steady-state junction potential and decreased (relative to when there is no 18C6 in solution) steady-state current.

That a steady-state current is, indeed, achieved in our experiments is shown by the data in Figure 8. These data also show that the K^+ –18C6 complex is transported into the conical nanopore because, in analogy to the α -HL case,¹⁵ a higher noise level is obtained in the presence of the complex. In the α -HL case, it has been suggested that higher noise is a consequence of nonspecific interactions between the complex and the protein nanopore.^{14,16}

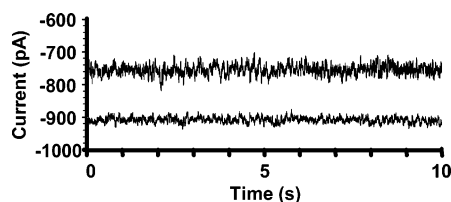


Figure 8. Current–time transients showing steady-state currents for a conical nanopore with mouth diameter ~ 1.5 nm, and with 1 M KCl as the electrolyte. The lower trace (larger negative current) is for 1 M KCl only. The upper trace is for 1 M KCl plus 10 mM 18C6 added to the solution facing the mouth of the nanopore.

Conclusions

We have shown that adding 18C6 to the electrolyte solution on one side of a conical nanopore membrane provides a way to rectify the ion current flowing through the nanopore. This chemical rectification is only observed when the cation of the electrolyte is complexed by 18C6, and when the mouth diameter of the conical nanopore is of molecular dimensions, in this case 1.5 nm. As shown in Figure 7, this chemical rectification can either augment or diminish the inherent electrostatic rectification observed with these small mouth-diameter nanopores. The extent of this chemical rectification increases with the concentration of 18C6 added to the electrolyte solution. We have interpreted these results using a model based on the formation of a junction potential at the membrane/solution interface. This junction potential arises because the transference number for the K^+ –18C6 complex in bulk solution is larger than its transference number in the mouth of the nanopore. These results have potential ramifications in controlling ion transport in nanofluidic channels, and in the development of nanofluidic circuits.⁴¹ These results also have implications for the design and development of synthetic nanopore-based sensors.¹²

Results analogous to those observed here were obtained when 18C6 was used to probe ion transport in a protein nanopore, α -hemolysin (α -HL). The similarity of the α -HL and conical nanopore results confirms that the mouth of the conical nanopore is truly of molecular dimensions. This is important because the α -HL nanopore has been used as a transducer in chemical and biosensing experiments.^{42–47} However, these prototype sensors entail immobilization of the α -HL in a planar bilayer membrane, and this construct is too fragile to provide a practical sensing device. The ultimate objective of our work is to make analogous biosensors based on abiotic conical nanopores of the type described here.¹²

Acknowledgment. This research was supported by the National Science Foundation and the Defense Advanced Research Projects Agency.

References and Notes

- (1) Cooper, G. M. *The Cell: A Molecular Approach*, 2nd ed.; Sinauer Associates: Sunderland, MA, 2000; pp 81–84, 476–491.
- (2) Hille, B. *Ion Channels of Excitable Membranes*, 3rd ed.; Sinauer Associates: Sunderland, MA, 2001; p 814.
- (3) Siwy, Z.; Apel, P.; Baur, D.; Dobrev, D. D.; Korchev, Y. E.; Neumann, R.; Spohr, R.; Trautmann, C.; Voss, K.-O. *Surf. Sci.* **2003**, 532–535, 1061–1066.
- (4) Siwy, Z.; Heins, E.; Harrell, C. C.; Kohli, P.; Martin, C. R. *J. Am. Chem. Soc.* **2004**, 126, 10850–10851.
- (5) Siwy, Z.; Gu, Y.; Spohr, H. A.; Baur, D.; Wolf-Reber, A.; Spohr, R.; Apel, P.; Korchev, Y. E. *Europhys. Lett.* **2002**, 60, 349–355.
- (6) Harrell, C. C.; Kohli, P.; Siwy, Z.; Martin, C. R. *J. Am. Chem. Soc.* **2004**, 126, 15646–15647.
- (7) Kasianowicz, J. J.; Brandin, E.; Branton, D.; Deamer, D. W. *Proc. Natl. Acad. Sci. U.S.A.* **1996**, 93, 13770–13773.
- (8) Bayley, H.; Martin, C. R. *Chem. Rev.* **2000**, 100, 2575–2594.
- (9) Siwy, Z.; Fulinski, A. *Phys. Rev. Lett.* **2002**, 89, 198103/1–198103/4.
- (10) Fleischer, R. L.; Price, P. B.; Walker, R. M. *Nuclear Tracks in Solids: Principles and Applications*; University of California Press: Berkeley, CA, 1975; p 605.
- (11) Siwy, Z.; Dobrev, D.; Neumann, R.; Trautmann, C.; Voss, K. *Appl. Phys. A* **2003**, 76, 781–785.
- (12) Siwy, Z.; Trofin, L.; Kohli, P.; Baker, L. A.; Trautmann, C.; Martin, C. R. *J. Am. Chem. Soc.* **2005**, 127, 5000–5001.
- (13) Steinle, E. D.; Mitchell, D. T.; Wirtz, M.; Lee, S. B.; Young, V. Y.; Martin, C. R. *Anal. Chem.* **2002**, 74, 2416–2422.
- (14) Bezrukov, S. M.; Kasianowicz, J. J. *Eur. Biophys. J.* **1997**, 26, 471–476.
- (15) Bezrukov, S. M.; Krasilnikov, O. V.; Yuldasheva, L. N.; Berezhkovskii, A. M.; Rodrigues, C. G. *Biophys. J.* **2004**, 87, 3162–3171.
- (16) Krasilnikov, O. V.; Bezrukov, S. M. *Macromolecules* **2004**, 37, 2650–2657.
- (17) Merzlyak, P. G.; Yuldasheva, L. N.; Rodrigues, C. G.; Carneiro, C. M. M.; Krasilnikov, O. V.; Bezrukov, S. M. *Biophys. J.* **1999**, 77, 3023–3033.
- (18) Pedersen, C. J. *J. Am. Chem. Soc.* **1967**, 89, 7017–7036.
- (19) Steed, J. W.; Atwood, J. L. *Supramolecular Chemistry: An Introduction*; John Wiley & Sons: New York, 2000; p 772.
- (20) Song, L.; Hobaugh, M. R.; Shustak, C.; Cheley, S.; Bayley, H.; Gouaux, J. E. *Science* **1996**, 274, 1859–1866.
- (21) Bard, A. J.; Faulkner, L. R. *Electrochemical Methods*, 2nd ed.; John Wiley & Sons: New York, 2001; pp 63–74.
- (22) Apel, P. Y.; Korchev, Y. E.; Siwy, Z.; Spohr, R.; Yoshida, M. *Nucl. Instrum. Methods Phys. Res., Sect. B* **2001**, 184, 337–346.
- (23) Trautmann, C.; Bruechle, W.; Spohr, R.; Vetter, J.; Angert, N. *Nucl. Instrum. Methods Phys. Res., Sect. B* **1996**, 111, 70–74.
- (24) Wolf-Reber, A. Aufbau eines Rasterionenleitwertmikroskops. Stromsfluktuationen in Nanoporen. Ph.D. Dissertation, University of Frankfurt, Frankfurt, Germany, 2002.
- (25) Nishizawa, M.; Menon, V. P.; Martin, C. R. *Science* **1995**, 268, 700–702.
- (26) Siwy, Z.; Fulinski, A. *Am. J. Phys.* **2004**, 72, 567–574.
- (27) Frensdorff, J. K. *J. Am. Chem. Soc.* **1971**, 93, 600–606.
- (28) Izatt, R. M.; Bradshaw, J. S.; Nielsen, S. A.; Lamb, J. D.; Christensen, J. J.; Sen, D. *Chem. Rev.* **1985**, 85, 271–339.
- (29) Miller, S. A.; Young, V. Y.; Martin, C. R. *J. Am. Chem. Soc.* **2001**, 123, 12335–12342.
- (30) Daiguji, H.; Yang, P.; Majumdar, A. *Nano Lett.* **2004**, 4, 137–142.
- (31) Sugawara, T.; Yudasaka, M.; Yokoyama, Y.; Fujiyama, T.; Iwamura, H. *J. Phys. Chem.* **1982**, 86, 2705–2709.
- (32) Kathawalla, I. A.; Anderson, J. L.; Lindsey, J. L. *Macromolecules* **1989**, 22, 1215–1219.
- (33) Coulter, W. H. Means for Counting Particles Suspended in a Fluid. U.S. Patent 2656508, 1953.
- (34) Bard, A. J.; Faulkner, L. R. *Electrochemical Methods*, 2nd ed.; John Wiley & Sons: New York, 2001; pp 66–67.
- (35) Freiser, H.; Fernando, Q. *Ionic Equilibria in Analytical Chemistry*; John Wiley & Sons: New York, 1963; p 25.
- (36) Bard, A. J.; Faulkner, L. R. *Electrochemical Methods*, 2nd ed.; John Wiley & Sons: New York, 2001; p 16.
- (37) Hille, B. *Ion Channels of Excitable Membranes*, 3rd ed.; Sinauer Associates: Sunderland, MA, 2001; pp 10–13.
- (38) Rothschild, L. J. *Biophys. Biochem. Cytol.* **1957**, 3, 103–110.
- (39) Bard, A. J.; Faulkner, L. R. *Electrochemical Methods*, 2nd ed.; John Wiley & Sons: New York, 2001; pp 168–176.
- (40) Zhang, B.; Zhang, Y.; White, H. S. *Anal. Chem.* **2004**, 76, 6229–6238.
- (41) Kuo, T.; Cannon, D. M.; Chen, Y.; Tulock, J. J.; Shannon, M. A.; Sweedler, J. V.; Bohn, P. W. *Anal. Chem.* **2003**, 75, 1861–1867.
- (42) Gu, L.-Q.; Braha, O.; Conlan, S.; Cheley, S.; Bayley, H. *Nature* **1999**, 398, 686–690.
- (43) Kasianowicz, J. J. *Dis. Markers* **2002**, 18, 185–191.
- (44) Howorka, S.; Nam, J.; Bayley, H.; Kahne, D. *Angew. Chem., Int. Ed.* **2004**, 43, 842–846.
- (45) Howorka, S.; Cheley, S.; Bayley, H. *Nat. Biotechnol.* **2001**, 19, 636–639.
- (46) Howorka, S.; Movileanu, L.; Braha, O.; Bayley, H. *Proc. Natl. Acad. Sci. U.S.A.* **2001**, 98, 12996–13001.
- (47) Gu, L.-Q.; Bayley, H. *Biophys. J.* **2000**, 79, 1967–1975.